AIP | Applied Physics Letters

Role of phase composition for electronic states in CH3NH3PbI3 prepared from CH3NH3I/PbCl2 solution

Atittaya Naikaew, Pongthep Prajongtat, Martha Ch. Lux-Steiner, Marisa Arunchaiya, and Thomas Dittrich

Citation: Applied Physics Letters **106**, 232104 (2015); doi: 10.1063/1.4922554
View online: http://dx.doi.org/10.1063/1.4922554
View Table of Contents: http://scitation.aip.org/content/aip/journal/apl/106/23?ver=pdfcov
Published by the AIP Publishing

Role of phase composition for electronic states in $CH_3NH_3PbI_3$ prepared from $CH_3NH_3I/PbCl_2$ solution

Atittaya Naikaew,[1,2] Pongthep Prajongtat,[1,2] Martha Ch. Lux-Steiner,[1] Marisa Arunchaiya,[2] and Thomas Dittrich[1,a)]
[1]*Helmholtz-Center Berlin for Energy and Materials, Institute of Heterogeneous Materials, Hahn-Meitner-Platz 1, D-14109 Berlin, Germany*
[2]*Department of Materials Science, Faculty of Science, Kasetsart University, Bangkok 10900, Thailand*

(Received 29 April 2015; accepted 4 June 2015; published online 10 June 2015)

Modulated surface photovoltage (SPV) spectra have been correlated with the phase composition in layers of $CH_3NH_3PbI_3$ ($MAPbI_3$) prepared from MAI and $PbCl_2$ and annealed at 100 °C. Depending on the annealing time, different compositions of $MAPbI_3$, $MAPbCl_3$, MACl, PbI_2, and an un-identified phase were found. It has been demonstrated that evaporation of MAI and HI is crucial for the development of electronic states in $MAPbI_3$ and that only the appearance and evolution of the phase PbI_2 has an influence on electronic states in $MAPbI_3$. With ongoing annealing, (i) a transition from p- to n-type doping was observed with the appearance of PbI_2, (ii) shallow acceptor states were distinguished and disappeared in n-type doped $MAPbI_3$, and (iii) a minimum of the SPV response related to deep defect states was found at the transition from p- to n-type doping. The results are discussed with respect to the further development of highly efficient and stable $MAPbI_3$ absorbers for solar cells.
[http://dx.doi.org/10.1063/1.4922554]

High solar energy conversion efficiencies have been demonstrated for solar cells with absorbers based on organic-inorganic hybrid lead halide perovskites, especially $CH_3NH_3PbI_3$ ($MAPbI_3$).[1,2] However, strong degradation makes the successful application of perovskite solar cells impossible to date. A better understanding of defect formation and degradation is crucial for the successful development of stable related solar cells.

Shallow acceptor and donor traps with low formation energy and flexible properties allowing for intrinsic p- and n-type doping have been observed by theoretical analysis.[3] This unusual defect physics of $MAPbI_3$ is in contrast, for example, to conventional $CuInSe_2$ thin-film absorbers for which the formation energy of acceptors is much lower than for donors.[4] It has been shown experimentally that an excess or deficit of CH_3NH_3I (MAI) in the perovskite precursor solution containing MAI and PbI_2 caused p- or n-type doping, respectively, of $MAPbI_3$.[5] Degradation of $MAPbI_3$ almost occurs at room temperature and leads to the formation of PbI_2.[6] The resulting $MAPbI_3/PbI_2$ interface is well passivated,[7] enables the transfer of electrons but blocks the transfer of holes.[8]

Mild annealing conditions at about 100 °C are applied for numerous preparation processes of $MAPbI_3$ layers used for high efficiency solar cells.[9,10] Furthermore, the addition of chlorine into the precursor led to improved performance of related solar cells.[11,12] The application of MAI or MACl and $PbCl_2$ or PbI_2 precursors causes coexisting phases and phase transformations involving the formation of $MAPbCl_3$, $MAPbI_3$, MACl, and PbI_2 as well as of un-identified phases.[9,10] $MAPbI_3$ was present as the dominant phase after all annealing times, and $MAPbCl_3$, MACl, and un-identified phases disappeared and PbI_2 appeared after long annealing times.[9,10] Therefore, the behavior of electronic states near and below the band gap of $MAPbI_3$ can be studied for samples with different phase compositions by following the preparation conditions described in the works of Song *et al.*[9] and Unger *et al.*[10]

In this work, $MAPbI_3$ has been prepared from MAI and $PbCl_2$ precursors with a mole ratio of 3 to 1 in *N*,*N*-dimethylformamide (DMF) and annealed at 100 °C for different times in order to investigate electronic properties of $MAPbI_3$ changing from p- to n-type doping in correlation with the phase composition. Grazing incidence x-ray diffraction (GIXRD) and modulated surface photovoltage (SPV) spectroscopy were applied for the characterization of the phase composition and of the electronic properties of the layers, respectively. In modulated SPV measurements, a semitransparent electrode (SnO_2:F) is gently pressed on a mica sheet which has been placed on the sample before. Therefore, modulated SPV measurements do not require any contact preparation so that the undisturbed $MAPbI_3$ samples were investigated after annealing. As remark, GIXRD and SPV measurements can be well correlated since the information depths are of the same order (penetration depth for GIXRD and diffusion length of photo-generated charge carriers[13] several 100 nm).

A 40 wt. % perovskite precursor solution was prepared by dissolving MAI (Dyesol) and $PbCl_2$ (Carl Roth Germany) with a 3:1 mole ratio in DMF (Sigma Aldrich). After stirring the precursor solution at 60 °C overnight, the solution was spin coated onto molybdenum coated glass substrates (1000 rpm for 10 s followed by 3000 rpm for 60 s). The layer thickness was about 300 nm. The layers were annealed at

a)Author to whom correspondence should be addressed. Electronic mail: dittrich@helmholtz-berlin.de

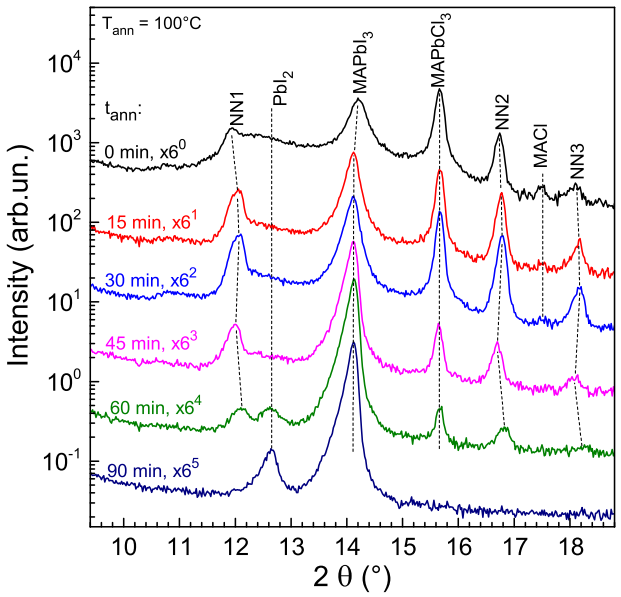

FIG. 1. GIXRD pattern of the as-deposited layer (black line) and of the layers annealed at 100 °C for 15, 30, 45, 60, and 90 min (red, blue, pink, green, and marine lines, respectively).

100 °C in a N_2-filled glovebox for 0, 15, 30, 45, 60, and 90 min. After annealing, the samples (size 25 × 25 mm^2) were cut into two separate samples and stored in nitrogen filled envelopes in the glovebox.

The modulated (modulation frequency 8 Hz) SPV measurements were carried out in vacuum ($2 \cdot 10^{-5}$ mbar) in the fixed capacitor arrangement[14] (see also the inset of Figure 2) in the day of sample preparation. Illumination was performed with a halogen lamp and a quartz prism monochromator (intensity on the sample about 0.8 mW/cm^2 at 830 nm). In-phase and phase-shifted by 90° SPV signals were detected with a high-impedance buffer and a double phase lock-in amplifier (EG&G 5210).

Figure 1 shows the GIXRD (angle of incidence 0.9°) patterns of the as-deposited layer and of the layers annealed for different times. As remark, little peaks related to molybdenum were still detected after layer deposition (not shown). The (110) diffraction peak of $MAPbI_3$ at around 14.22° or 14.12° (Ref. 15) appeared for the as-deposited and for all annealed samples, respectively. The peak height at 14.12° increased with the increase in annealing time up to 60 min and decreased slightly for the longer annealing time. The (100) diffraction peak of $MAPbCl_3$ at around 15.67° (Ref. 16) increased with the increase in annealing time up to 30 min, decreased with further increasing annealing time, and disappeared for the sample annealed for 90 min. The fact that the peak positions at 14.12° and 15.57° remained constant gave evidence for segregation of the pure $MAPbI_3$ and $MAPbCl_3$ phases. A tiny diffraction peak at 17.5° related to MACl[10] could be observed for the as-deposited sample and disappeared for annealing times above 30 min. The (001) diffraction peak of PbI_2 at 12.65° (Ref. 16) appeared after annealing for 60 min and increased strongly after annealing for 90 min. The un-identified diffraction peaks at around 12.0°, 16.7°, and 18.1°, denoted by NN1, NN2, and NN3 in Figure 1, respectively, were probably related to ongoing crystallization of precursors with a high amount of residual

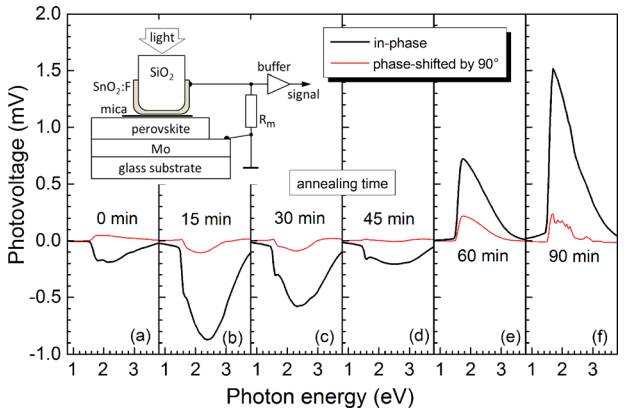

FIG. 2. Modulated in-phase (thick black lines) and phase-shifted by 90° (thin red lines) SPV spectra for the as-deposited sample (a) and for the samples annealed for 15, 30, 45, 60, and 90 min ((b)-(f), respectively). The inset shows a schematic of the measurement configuration.

solvent decreasing for annealing times longer than 30 min and disappearing after annealing for 90 min. The decrease in the amount of $MAPbCl_3$ and MACl was caused by evaporation of MACl.[9] The decrease of the amount of $MAPbI_3$ and the increase of the amount of PbI_2 were caused by ongoing evaporation of MAI.

Figure 2 shows the in-phase (x-signal) and phase-shifted by 90° (y-signal) SPV spectra of the as-deposited sample (a) and of the samples annealed for 15, 30, 45, 60, and 90 min ((b)–(f), respectively). As remark, the x- and y-signals are related to the responses following fast or slowly, respectively, in relation to the modulation period. All samples showed the dominant onset of SPV signals at about 1.5 eV, i.e., at the band gap of $MAPbI_3$.[13] This is in agreement with the existence of the $MAPbI_3$ phase detected in the XRD measurements.

The x-signals were negative for the as-deposited sample and for the samples annealed for 15, 30, and 45 min and positive for the samples annealed for 60 and 90 min. As a remark, a negative (positive) sign of the x-signals means that photo-generated electrons are separated preferentially towards the external surface (internal interface). The surface regions of moderately doped semiconductors are in depletion. Therefore, the change of the sign of the x-signals marked the change from p- to n-type doped $MAPbI_3$.

The change of the sign of the x-signals coincided with the appearance of the PbI_2 phase, whereas the $MAPbCl_3$ and the un-identified phases were still present after annealing for 60 min (see Figure 1). As a remark, a signature of the band gap of PbI_2 (around 2.3 eV[7]) just appeared in the spectra of the first derivative of the x-signals. Intrinsic n-type doping of $MAPbI_3$ was assigned to a deficiency of MA and I leading preferentially to interstitials of MA and vacancies of I which have the lowest formation energies.[3] Self-doping in $MAPbI_3$ by excess (p-type) or deficiency (n-type) of MA and I has been demonstrated by Hall-effect measurements.[5] As a conclusion, the appearance of PbI_2 at the surface of $MAPbI_3$ is a clear indication for the deficiency of MA and I in the region near the interface and therefore for n-type doping of $MAPbI_3$.

The sign of the y-signals was positive for the as-deposited sample and changed to negative for the samples

annealed for 15 and 30 min (photon energies between 1.6 and 3.2 eV); i.e., the x- and y-signals got the same sign. The x- and y-signals had also the same sign for the samples annealed for 60 and 90 min. As remark, the x- and y-signals had opposite signs for excitation of photo-generated charge carriers from defect states (photon energies below 1.55 eV).

The same sign of x- and y-signals means that there are two mechanisms of charge separation with opposite direction.[17] Evaporation of MACl and later of MAI starts with beginning annealing. Therefore, annealing leads to the formation of defect states near the surface of $MAPbI_3$ at which photo-generated holes can be trapped. Similarly, decomposition of $MAPbI_3$ at the $MAPbI_3/PbI_2$ interface leads to the formation of defect states at which electrons can be trapped.

The negative and positive x-signal heights have a maximum at 2.4 and 1.7 eV for the samples annealed for 15 and 90 min, respectively. The x-signals at 1.7 and 2.4 eV increased from −0.15 and −0.17 for the as-deposited sample to −0.50 and −0.87 mV, respectively, for the sample annealed for 15 min. This strong increase correlated with the increase of the XRD pattern for $MAPbI_3$ and was therefore related to ongoing formation of $MAPbI_3$.

The x-signals at 1.7 and 2.4 eV decreased to −0.3 and −0.57 and to −0.15 and −0.2 mV for the samples annealed for 30 and 45 min, respectively. At the same time, MACl disappeared. The decrease of the negative x-signals was related to the ongoing evaporation of MACl and MAI and therefore to the decrease of the concentration of acceptors.

The x-signals at 1.7 and 2.4 eV increased from 0.71 and 0.44 mV for the sample annealed for 60 min to 1.73 and 0.79 mV, respectively, for the sample annealed for 90 min. The increase of the positive x-signals was related to the ongoing evaporation of MAI and formation of PbI_2 and therefore to the increase of the concentration of donors.

A shoulder or little peak very close to the band gap of $MAPbI_3$ can be well distinguished in the spectra of the x-signals for the as-deposited samples and for the samples annealed for 15, 30, and 45 min, i.e., for the p-type doped samples. The disappearance of the related peak or shoulder in the n-type doped sample gave evidence for excitation of electrons from shallow acceptor states such as lead vacancies or iodine interstitials (have low formation energy and electronic states slightly above the valence band edge[3] into the conduction band of p-type doped samples. Furthermore, one has to keep in mind that a high density of shallow acceptors can distort the onset energy of the SPV spectrum. The shallow donors in n-type doped $MAPbI_3$ with low formation energy (MA interstitial and iodine vacancy[3]) have states within the conduction band what makes them difficult to be distinguished.

The significance of deep defect states can be described, for example, by the ratio of the PV amplitudes, i.e., the square root of the sum of the squared x- and y-signals, measured at 1.1 and at 1.7 eV ($R_{1.1\,eV}/R_{1.7\,eV}$). Figure 3 summarizes the dependence of $R_{1.1\,eV}/R_{1.7eV}$ on the annealing time together with the regions of the phases detected by XRD. For the as-deposited sample and for the samples annealed for 15, 30, and 45 min, the value of $R_{1.1\,eV}/R_{1.7eV}$ increased with increasing annealing time. The value of $R_{1.1\,eV}/R_{1.7eV}$ dropped strongly down by more than one order of magnitude for the sample annealed for 60 min and increased again for the sample annealed for 90 min. The minimum of the value of $R_{1.1\,eV}/R_{1.7eV}$ correlated with the transition from p-type to n-type doping and with the appearance of PbI_2.

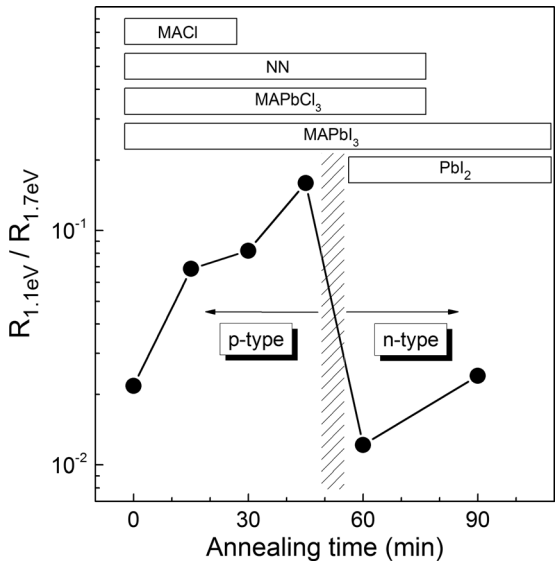

FIG. 3. Dependence of the ratio of the PV amplitudes measured at 1.1 and at 1.7 eV on the annealing time. The inserted boxes mark the regions of phases detected by XRD.

Evaporation of MAI caused the formation of structural defects near the surface of p-type doped $MAPbI_3$. Structural defects near the surface of $MAPbI_3$ merged to a new phase, i.e., PbI_2, at the transition point to n-type doping. With further annealing, HI, having also low dissociation energy,[6] evaporated and created damage of the lattice near the developing $MAPbI_3/PbI_2$ interface.[6] This result shows that there is only a narrow window for optimization of the electronic properties of $MAPbI_3$ with respect to doping and a minimum of defect states.

The phase composition practically does not have influence on the electronic states being important for the electronic properties of $MAPbI_3$ excluding the formation of PbI_2 being an indication for n-type doping. The strong dependence of the doping of $MAPbI_3$ on continued evaporation of MAI and HI makes the reproducibility of electronic properties of $MAPbI_3$ rather challenging in relation to the preparation and to the stability of solar cells with $MAPbI_3$ absorbers. Therefore, sinks for MAI and/or HI have to be minimized or avoided for reaching a high long-term stability of solar cells with $MAPbI_3$ absorbers. One opportunity can be, for example, the dedicated stabilization of bond configurations at interfaces with $MAPbI_3$, for example, by introducing ammonium valeric acid iodide.[15] Another opportunity can be the formation of dense interfaces between $MAPbI_3$ and inorganic contact layers. As a remark, it seems rather harsh to avoid diffusion of HI in polymer layers and to get high long-term stability of solar cells with $MAPbI_3$ absorbers including interfaces between $MAPbI_3$ and organic contact layers. However, detailed investigations on the stability of interfaces with $MAPbI_3$ are required, whereas SPV measurements can be very helpful.

As a remark, surface coverage is a major issue for the performance of solar cells based on $MAPbI_3$ as stated, for example, by Eperon.[18] In this work, the coverage of Mo with $MAPbI_3$ was above 95%, i.e., pinholes could not be avoided yet. However, the obtained SPV results are not affected by pinholes. Furthermore, the evolution and passivation of defects depend sensitively on the ambient. For example, annealing in air resulted in less disorder of $MAPbI_3$ in comparison to annealing in nitrogen,[19] whereas the decomposition rates are strongly enhanced in air. This is not surprising since adsorbed water molecules can decompose at semiconductor surfaces and resulting hydrogen or hydroxide can passivate defects or enhance corrosion, respectively. It can be expected that the increased decomposition rate of $MAPbI_3$ in humid ambient will lead to a reduced onset time of the transition from p- to n-type doping.

The authors are grateful to the Development and Promotion of Science and Technology Talent Project (DPST, Thailand, P.P.), to the Graduate School of the Kasetsart University (Graduate Study Research Scholarship for International Publications Year 2013, A.N.), to the Faculty of Science of the Kasetsart University (Bilateral Research Cooperation -BRC-, A.N. and M.A.) and to the Kasetsart University Research and Development Institute (KURDI, M.A.). Further, the authors are grateful to the reviewers for helpful remarks enriching the discussion.

[1]N. J. Jeon, J. H. Noh, Y. C. Kim, W. S. Yang, S. Ryu, and S. I. Seok, Nat. Mater. **13**, 897 (2014).
[2]H. Zhou, Q. Chen, G. Li, S. Luo, T.-b. Song, H.-S. Duan, Z. Hong, J. You, Y. Liu, and Y. Yang, Science **345**, 542 (2014).
[3]W.-J. Yin, T. Shi, and Y. Yan, Appl. Phys. Lett. **104**, 063903 (2014).
[4]S. B. Zhang, S.-H. Wei, A. Zunger, and H. Katayama-Yoshida, Phys. Rev. B **57**, 9642 (1998).
[5]Q. Wang, Y. Shao, H. Xie, L. Lyu, X. Liu, Y. Gao, and J. Huang, App. Phys. Lett. **105**, 163508 (2014).
[6]I. Deretzis, A. Alberti, G. Pellegrino, E. Smecca, F. Giannazzo, N. Sakai, T. Miyasaka, and A. La Magna, Appl. Phys. Lett. **106**, 131904 (2015).
[7]T. Supasai, N. Rujisamphan, K. Ullrich, A. Chemseddine, and T. Dittrich, Appl. Phys. Lett. **103**, 183906 (2013).
[8]V. Somsongkul, F. Lang, A. R. Jeong, M. Rusu, M. Arunchaiya, and T. Dittrich, Phys. Status Solidi (RRL) **08**, 763 (2014).
[9]T.-B. Song, Q. Chen, H. Zhou, S. Luo, Y. Yang, and J. You, Nano Energy **12**, 494 (2015).
[10]E. L. Unger, A. R. Bowring, C. J. Tassone, V. L. Pool, A. Gold-Parker, R. Cheacharoen, K. H. Stone, E. T. Hoke, M. F. Toney, and M. D. McGehee, Chem. Mater. **26**, 7158 (2014).
[11]S. D. Stranks, G. E. Eperon, G. Grancini, C. Menelaou, M. J. P. Alcocer, T. Leijtens, L. M. Herz, A. Petrozza, and H. J. Snaith, Science **342**, 341 (2013).
[12]C. Wehrenfennig, G. E. Eperon, M. B. Johnston, H. J. Snaith, and L. M. Herz, Adv. Mater. **26**, 1584 (2014).
[13]S. A. Bretschneider, J. Weickert, J. A. Dorman, and L. Schmidt-Mende, APL Mater. **2**, 040701 (2014).
[14]V. Duzhko, V. Y. Timoshenko, F. Koch, and T. Dittrich, Phys. Rev. B **64**, 075204 (2001).
[15]A. Mei, X. Li, L. Liu, Z. Ku, T. Liu, Y. Rong, M. Xu, M. Hu, J. Chen, Y. Yang, M. Grätzel, and H. Han, Science **345**, 295 (2014).
[16]B.-W. Park, B. Philippe, T. Gustafsson, K. Sveinbjörnsson, A. Hagfeldt, E. M. J. Johansson, and G. Boschloo, Chem. Mater. **26**, 4466 (2014).
[17]P. Prajongtat and T. Dittrich, J. Phys. Chem. C **119**, 9926 (2015).
[18]G. E. Eperon, V. M. Burlakov, P. Docampo, A. Goriely, and H. J. Snaith, Adv. Funct. Mater. **24**, 151 (2014).
[19]S. Pathak, A. Sepo, A. Sadhanala, F. Deschler, A. Haghighirad, N. Sakai, K. C. Goedel, S. D. Stranks, N. Noel, M. Price, S. Hüttner, N. A. Hawkins, R. H. Friend, U. Steiner, and H. J. Snaith, ACS Nano **9**, 2311 (2015).